ANALYTICAL, NUMERICAL, AND EXPERIMENTAL METHODS FOR THROUGH-THE-WALL RADAR IMAGING

Mojtaba Dehmollaian and Kamal Sarabandi

Radiation Laboratory,
Department of Electrical Engineering and Computer Science,
The University of Michigan, Ann Arbor

ABSTRACT

In this paper a physics-based approach for image formation of targets behind complex wall structures is presented. Analytical and numerical techniques are used for the development of forward scattering models which are then exploited in construction of matched filters for ultra-wideband synthetic aperture radars operating over a wide rang of incidence angles. Special scattering models for different wall types including cinder block and reinforced concrete walls are presented using efficient numerical and approximate analytical techniques. These allow for construction of SAR images as well as development of a refocusing algorithm. An experimental ultra-wideband radar is set up in the laboratory environment for the evaluation of the models presented. Also, a radar measurement configuration is proposed that allows for elimination of direct reflection from the walls.

Index Terms— Ultra wideband SAR, through-wall imaging, Electromagnetic(EM) Modeling

1. INTRODUCTION

The ability to see through walls can make many civilian, law enforcement and military applications possible [1], [2]. For example earthquake rescue operations, police search operations, and threat assessment situations all require the ability to detect and identify objects hidden behind walls. Synthetic aperture radar (SAR) systems is used in this paper to image the interior of buildings and identify the signature of inside targets. Since the transmissivity of the wall is a function of both frequency and incident angles, the effect of the wall on the target image becomes significant. Therefore, there is an emergent need for development of physics-based models for computation of scattering from and transmission through complex wall structures.

At low microwave frequencies, we may categorize walls into two groups: 1) homogenous walls such as brick, adobe, and poured concrete walls and 2) inhomogeneous walls, such as cinder block, drywalls and re-enforced concrete walls. For homogenous walls dielectric slab models can predict the transmission and reflection coefficient properties of the walls with reasonable accuracies. On the other hand, for inhomogeneous walls where the spatial inhomogeneities are comparable to the wavelength, detailed models are needed. Walls constructed of concrete cinder blocks or reinforced concrete or combination of studs and drywalls used in the building interiors are modeled by periodic structures. Wave interaction with such periodic structures excite Floquet modes at frequencies where the periodicity is larger than half a wavelength. Such structures scatter an incoming ray into many directions and complicate imaging algorithms.

Using the comprehensive models developed for characterizing the EM properties of different walls, construction of SAR images as well as development of a refocusing algorithm is possible.

2. FORMULATIONS

Figure 1 shows a scenario of target detection behind a wall using a SAR system. As shown, the ultra-wideband transceiver antenna moves along the scan line with length of L and collects the backscattered field for different frequency and observation points. Here, the scan line is chosen to be parallel to the wall, located at x_o, and a point target is placed at $-x_s$ behind the wall. Using the standard focused SAR imaging technique and assuming $e^{-i\omega t}$ time convention, the target image is computed by

$$\tilde{S}(\bar{r}) = \frac{1}{N_p N_f} \sum_{m=1}^{N_f} \sum_{n=1}^{N_p} E_r^t(\bar{r}_n, k_m)\, R_n^2(\bar{r}_n, \bar{r})\, e^{-2ik_m R_n(\bar{r}_n,\bar{r})}, \quad (1)$$

where $R_n(\bar{r}_n, \bar{r}) = |\bar{r} - \bar{r}_n| = \sqrt{(x-x_n)^2 + (y-y_n)^2}$ is the distance from n^{th} observation point and k_m is the m^{th} wave constant, which is equal to $2\pi f_m/c$, where c is the speed of light in free space and f_m is the m^{th} frequency point. In (1), N_p and N_f are the number of observation and frequency points, respectively.

The received signal from the point target E_r^t is given by

$$E_r^t(\bar{r}_n, k_m) = \frac{G\lambda}{4\pi} \frac{e^{2ik_m R_{0n}}}{R_{0n}^2} S(k_m)\, T^2(\bar{r}_n, \bar{r}_s, k_m) \quad (2)$$

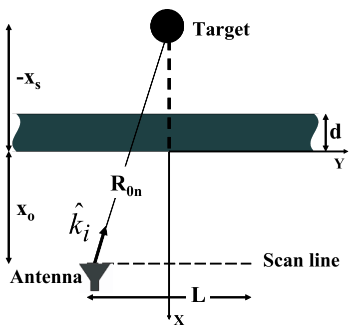

Fig. 1. Target imaging/detection by using a moving transceiver antenna.

where $R_{0n} = |\overline{r}_n - \overline{r}_s|$, G is the antenna gain, λ is the wavelength, $S(k_m)$ is the point target backscattering response. Along the synthetic aperture, it is assumed that the target is illuminated by the main beam of the antenna and that the antenna pattern does not significantly change inside that beam. Therefore, the gain angular dependance is neglected. The transmissivity matrix T can be measured or computed by EM models.

2.1. Homogenous Walls

Building walls such as brick, adobe, and poured concrete walls can be modeled by homogeneous dielectric slabs. The matrix T is a diagonal in the principal coordinate system and is equal to Diag[t_v,t_h] where the expressions for the transmission coefficient $t_{v/h}$ respectively for vertically or horizontally polarized incident waves through a dielectric slab are given in terms of the wall thickness d and relative permittivity ϵ_r.

To demonstrate the target imaging experimentally a small trihedral corner reflector, with pentagonal panel geometry is used as a point target behind a poured concrete wall with thickness of 20 cm. The back corner of the trihedral (scattering phase center) is at x = -0.71 m and at the same hight as that of the receiver antenna, 1.28 m above the ground plane. The transmitting and receiving antennas are on the other side of the wall, mounted on a vertical wooden rod and moving along a scan line with length L =95.88 cm (see Fig. 2). The transmitting antenna is attached about D_A = 0.25 m below the receiving antenna on the wooden rod. The apertures of both antennas are about D_W = 0.45 m away from the wall . The frequency of operation is from 1-2.5 GHz, the step frequency is 12.5 MHz, and the transceiver moves along the scan line with spacing of 2.04 cm. To reduce the effect of reflection from the wall, background subtraction is performed.

Using standard SAR imaging, the normalized target image is shown in Fig. 3. To compare the target image and its ideal image another measurement is performed when the wall is removed. It is observed that the standard target imaging locates the target further back from its actual position and the cross-range resolution is significantly decreased. The image is compensated for the effect of the wall using only the phase of transmission coefficients. That is in computation of (1), E_r^t is replaced by $E_r^t e^{-2i\angle T}$. The results are shown in Fig. 4. The compensated image is in close agreement with the target image when there is no wall.

Fig. 2. Measurement setup.

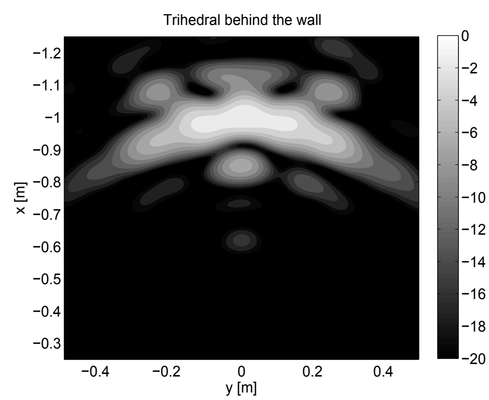

Fig. 3. Trihedral image using standard focused SAR imaging technique.

2.2. Inhomogenous Walls

A hybrid finite difference time domain (FDTD) and Ray optics approximation for analyzing the cinder block walls was presented by the authors before. Basically, the incident field on each block of the wall is approximated locally by a plane wave proportional to the ray emanated from the transmitting antenna. In this case, the radiated field can be viewed as a set of rays. The fields inside each block are then approximated as if the block was located inside an infinite structure of periodic blocks illuminated by a plane wave. Using this assumption, the field inside each block, is computed for different incident

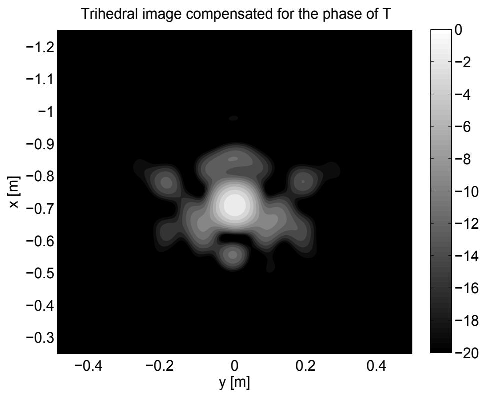

Fig. 4. Refocused image of the trihedral.

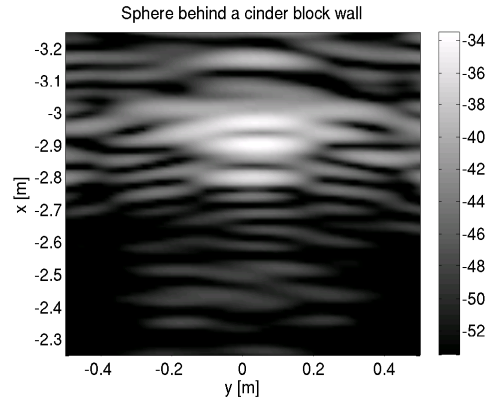

Fig. 5. Image of the sphere behind the cinder block wall.

angles employing FDTD technique. Next, the dielectric wall is replaced with polarization currents. Having the equivalent currents at discretized points inside each block the scattered field at any observation point can be obtained using the far-field expression of the dyadic Green's function.

Here experimental data are illustrated to address the effect of cinder block walls. To demonstrate the effect of the transmission through the cinder block walls on a point target image experimentally a metallic sphere with a diameter of 30.48 cm is used as a target and placed at about 2.7 m behind a cinder block wall. The size of each block is 19.5 cm $\times$ 39.5 cm $\times$ 19 cm and the overall size of the wall is 2.37 m $\times$ 1.90 m. The antennas are located at 0.9 m in front of the wall. They move along a 1 m scan-line with step of 2.04 cm. The target image is computed using the backscattered data collected for the frequency range of 1-4 GHz and the step frequency of 12.5 MHz. The result is illustrated in Fig.5. As shown, multiple focused points along the range are generated in the image.

To refocus the image, another measurement is carried out to estimate the transmissivity of the wall. That is the transmitting antenna is placed at the target position and the receiving antenna is kept in front of the wall at its original position. For different position of the receiving antenna, S12 is measured for two cases, one with the wall and one without the wall. The transmissivity is estimated as the ratio of the two recorded signals. The backscatter data is compensated for the phase of measured transmissivity and the result is shown in Fig.6. As shown, the image is well focused and the point target image is reconstructed.

The problem of EM scattering from reinforced concrete walls is considered and an approximate analytical solution is obtained. This is accomplished by invoking the thin wire approximation and assuming only axial induced currents on the metallic rebars, embedded in the concrete. This in conjunction with closed-form expressions for the Green's function of the problem leads to an analytical solution for the reflection

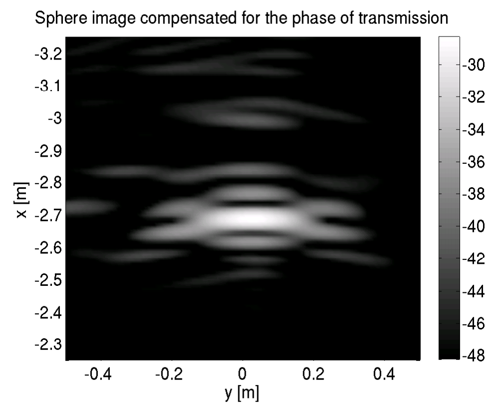

Fig. 6. Image of the sphere compensated for the phase of measured transmissivity.

and transmission coefficient of all Bragg modes of an arbitrary incident plane wave. The Green's function of the 2-D periodic structure of crossed rebar embedded in a concrete layer is approximated by the superposition of Green's function of two orthogonal 1-D periodic structures and a procedure similar to the vertical rebar structure is followed to arrive at a simple solution. Simulation results are verified using an independent formulation based on FDTD.

Here, as an example the zeroth order transmission coefficient of a vertical rebar wall as function of frequency is calculated using the approximate analytical approach and compared with the exact FDTD numerical computation (see Fig. 7). The wall thickness is 20.4 cm, metal thickness is 2.4 cm, and periodicity of rebars is 30.6 cm. The relative dielectric constant of the concrete is $\epsilon_r = 6$ and its conductivity is $\sigma = 0.01$. Position of metallic rods is at the middle of the dielectric (i.e. 10.2 cm). Excellent agreement is shown in Fig. 7.

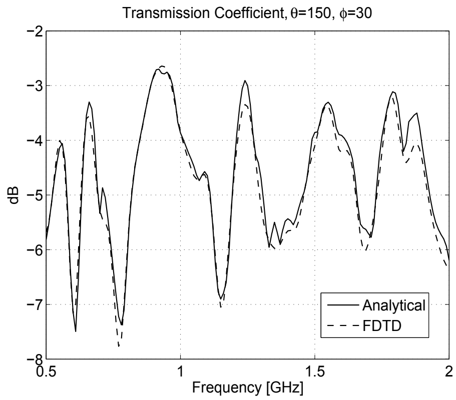

Fig. 7. Magnitude of co-polarized transmission coefficient of the vertical rebar concrete wall at oblique incidence angle (θ=150, ϕ=30) for horizontal polarization of incident field.

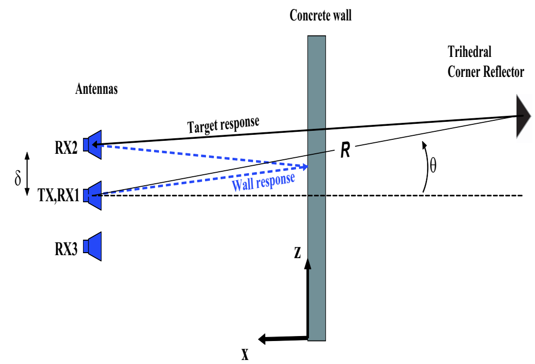

Fig. 8. Target imaging/detection using difference signals.

2.3. Through-Wall Imaging Using Difference Signals

In order to increase the signal to clutter ratio, it is of interest to suppress the reflection from the wall using a proper measurement setup. This is accomplished using three antennas shown in Fig. 8. Let us suppose all antennas are receivers and one is transmitter (i.e. the one in the middle) . A difference signal $\Delta E_r = E_{r3} - E_{r2}$ is computed by subtracting the signal of upper receiver from that of the lower receiver. Because of the symmetry, the contribution of the reflection from the wall in the difference signal is suppressed. To show the performance of this system a simulation is performed. A trihedral corner reflector (with sides of 18 cm) is placed at height of $z = 3.5$ m at distance of $-x_s$=5 m behind a poured concrete wall with thickness of 20 cm. The antennas 1, 2, and 3 are respectively located at height of z =2.0, 2.2, and 1.8 meters. The scanning track is 1 m long and located at x_o=5 m. An image based on summation of received signals $\Sigma E_r = E_{r1} + E_{r2}\, e^{+ik_m\delta\ sin(\theta)} + E_{r3}\, e^{-ik_m\ \delta\ sin(\theta)}$ is computed where the result is shown in Fig. 9. Here frequency of operation is from 1-2.5 GHz, and permittivity of the wall is 6. The image using the difference signal ΔE_r is computed and shown in Fig. 10. In comparison, the signal to clutter ratio is significantly improved employing the interferometric signal.

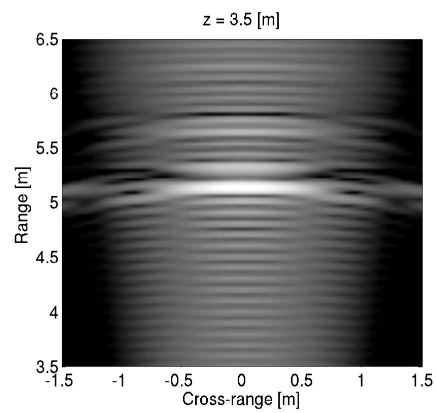

Fig. 9. The ΣE image of trihedral corner reflector.

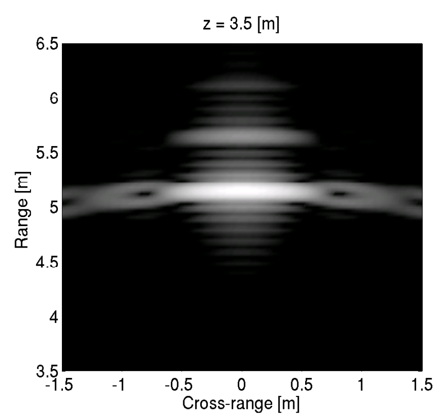

Fig. 10. The ΔE image of trihedral corner reflector.

3. REFERENCES

[1] David D. Ferris Jr. and Nicholas C. Currie, *A Survey of Current Technologies for Through-the-Wall Surveillance (TWS)*, proc. SPIE, Vol. 3577, pp. 62-72, Jan. 1999.

[2] Fauzia Ahmad, Moeness Amin, and Saleem A. Kassam, *Synthetic Aperture Beamformer for Imaging Through a Dielectric Wall*, IEEE Trans. on Aerospace and Electronic Systems, Vol. 41, No. 1, pp. 271-283, Jan. 2005.